Chronic Sleep Fragmentation Induces Endothelial Dysfunction and Structural Vascular Changes in Mice

Alba Carreras, PhD; Shelley X. Zhang, MD, MS; Eduard Peris, MSc; Zhuanhong Qiao, PhD; Alex Gileles-Hillel, MD; Richard C. Li, MD, PhD; Yang Wang, MD, PhD; David Gozal, MD

Section of Pediatric Sleep Medicine, Department of Pediatrics, Comer Children's Hospital, Pritzker School of Medicine, The University of Chicago, Chicago, IL

Study Objectives: Sleep fragmentation (SF) is a common occurrence and constitutes a major characteristic of obstructive sleep apnea (OSA). SF has been implicated in multiple OSA-related morbidities, but it is unclear whether SF underlies any of the cardiovascular morbidities of OSA. We hypothesized that long-term SF exposures may lead to endothelial dysfunction and altered vessel wall structure.

Methods and Results: Adult male C57BL/6J mice were fed normal chow and exposed to daylight SF or control sleep (CTL) for 20 weeks. Telemetric blood pressure and endothelial function were assessed weekly using a modified laser-Doppler hyperemic test. Atherosclerotic plaques, elastic fiber disruption, lumen area, wall thickness, foam cells, and macrophage recruitment, as well as expression of senescence-associated markers were examined in excised aortas. Increased latencies to reach baseline perfusion levels during the post-occlusive period emerged in SF mice with increased systemic BP values starting at 8 weeks of SF and persisting thereafter. No obvious atherosclerotic plaques emerged, but marked elastic fiber disruption and fiber disorganization were apparent in SF-exposed mice, along with increases in the number of foam cells and macrophages in the aorta wall. Senescence markers showed reduced TERT and cyclin A and increased p16INK4a expression, with higher IL-6 plasma levels in SF-exposed mice.

Conclusions: Long-term sleep fragmentation induces vascular endothelial dysfunction and mild blood pressure increases. Sleep fragmentation also leads to morphologic vessel changes characterized by elastic fiber disruption and disorganization, increased recruitment of inflammatory cells, and altered expression of senescence markers, thereby supporting a role for sleep fragmentation in the cardiovascular morbidity of OSA.

Keywords: sleep apnea, endothelial function, atherosclerosis, cell senescence

Citation: Carreras A, Zhang SX, Peris E, Qiao Z, Gileles-Hillel A, Li RC, Wang Y, Gozal D. Chronic sleep fragmentation induces endothelial dysfunction and structural vascular changes in mice. *SLEEP* 2014;37(11):1817-1824.

INTRODUCTION

OSA is a highly prevalent disorder affecting 4% to 10% of all adults and 2% to 4% of all children, and has emerged as an important health problem due to the extensive cardiovascular, metabolic, and CNS morbidities that have been associated with this disease when left untreated.[1-4] OSA is characterized by repetitive obstructions of the upper airway during sleep that result in intermittent hypoxia (IH), increased inspiratory efforts, and sleep fragmentation (SF). Initial studies using IH in animal models led to recognition of the major role played by episodic events of hypoxia and re-oxygenation in OSA-induced cardiovascular morbidity.[5-7] However, the potential role of SF has not been explored as extensively, such that it still remains unclear to what extent the recurring arousals and sleep disruption that characterize OSA contribute to the cardiovascular phenotype of this frequent disorder.[8,9]

We have recently developed a rodent model in which SF is implemented using an automated system that is not associated with increases in stress hormones, and that enables preservation of the spontaneous social and feeding behaviors in a human contact-free environment.[10-12] Using this approach, it became apparent that chronic SF during the daylight hours, i.e., the preferential period during which sleep occurs in mice leads to increased sleep propensity in the absence of sleep curtailment and to cognitive deficits via activation of inflammatory and oxidative pathways.[13-15] We reasoned that since such pathways are intimately involved in endothelial dysfunction and atherogenesis, long-term SF may promote the occurrence of vascular injury. Here, we show that indeed prolonged SF induces alterations in systemic blood pressure (BP) and in post-occlusive vascular reactivity and changes in arterial wall cellular substrates and overall structure.

MATERIALS AND METHODS

Animals

Adult male C57BL/6J mice from Jackson Laboratories (8-week old, ~22 g; Bar Harbor, ME, USA), were housed in groups of 5 (to prevent isolation stress) in standard clear polycarbonate cages and allowed to acclimatize to their surroundings. Mice were fed normal chow diet and water *ad libitum* and maintained in a 12-h light/dark cycle (light on 07:00 to 19:00) at a constant temperature (24 ± 1°C). A total of 30 mice (15/experimental group) were randomly assigned to SF exposures or CTL conditions for a period of 20 weeks. Expression of senescence-associated markers and other localized structural changes were examined in excised aortas after 20 weeks of SF exposures. Endothelial function was assessed weekly, and aorta lumen area, wall thickness, elastic fiber disruption grade, atherosclerotic plaques, and immune cell recruitment blood pressure over 20 weeks of SF using telemetry. At the end of

Submitted for publication January, 2014
Submitted in final revised form April, 2014
Accepted for publication May, 2014
Address correspondence to: David Gozal, MD, Department of Pediatrics, Pritzker School of Medicine, The University of Chicago, 5721 S. Maryland Avenue, MC8000, K160, Chicago, IL 60637-1470; Tel: (773) 702-3360; Fax: (773) 702-4523; E-mail: dgozal@uchicago.edu

the experimental procedures, mice were sacrificed by cervical dislocation. A separate set of mice served to test systolic and diastolic BP at several time points during the SF experimental period. Animal experiments were performed according to protocols approved by the IACUC of the University of Chicago and are in close agreement with the National Institutes of Health Guide in the Care and Use of Animals. All efforts were made to minimize animal suffering and to reduce the number of animals used.

Sleep Fragmentation

The SF device used to induce sleep disruption events has been previously described.[10,11,16] Briefly, it employs intermittent tactile stimulation using a near-silent motorized horizontal bar sweeping just above the cage floor from one side to the other. Since on average, 30 episodes of arousal per hour occur in patients with severe OSA (i.e., every 2 min), our aim was to mimic closely the severe disease condition, and thus, a 2-min interval between each sweep was implemented during the light period (07:00 to 19:00). SF was performed by switching on the sweeper to a timer mode in the cage. In this mode, the sweeper required around 9 sec to sweep the floor of the cage one way. When it reached the end of the cage, a relay engaged the timer which paused for ~110 sec before enabling the sweeper to move in the opposite direction. Between the 2 intervals, the animal remained undisturbed. During sweeper motion, animals would need to step over the sweeper, and then continue with their unrestrained behavior. SF exposure lasted for 20 weeks, during which mice had *ad libitum* access to food and water. Of note, this method prevents the need for human contact and intervention, minimizes physical activity during the entire sleep disruption procedure, does not require social isolation, and is associated with unchanged levels of stress hormones.[10,11,16]

Endothelial Function

Endothelial function was assessed weekly using a modified hyperemic test after 5-min cuff-induced occlusion of the dorsal tail vein. All tests were performed at the same time of the day (middle of the light period). A laser Doppler sensor (Periflux 5000 System, Perimed AB, Järfälla, Sweden) was applied on the dorsal tail vein, and the tail was gently immobilized. This site was chosen to minimize the effects of motion artifacts and includes a very vascular core that enables appropriate detection of the laser Doppler signal. Once blood flow in the tail became stable, 5 min of baseline blood flow were registered. Then, the pressure within an inflatable cuff placed at the origin of the tail was raised to suprasystolic values for 5 min, during which blood flow was reduced to undetectable levels. After the occlusion period, the cuff was rapidly deflated and the hyperemic response was measured. Although vascular perfusion slightly varies from mouse to mouse, all blood flow measurements were extrapolated to baseline perfusion values before cuff occlusion, such that analysis of reperfusion kinetics was based on temporal trajectory. Commercially available software (Perimed AB, Järfälla, Sweden) allowed for unbiased estimates of the time to peak regional blood flow response after the occlusion period and time to reach baseline levels after occlusion, the latter being considered as representative of the post-occlusion hyperemic response, an index of endothelial function.[17,18]

Implantation of Telemetric Transmitters for Blood Pressure Measurements

Surgical implantation of telemetric device for recordings of systemic BP was performed under sterile conditions and general anesthesia with isoflurane. The HD-X11 telemetric transmitter (Data Sciences International, St. Paul, Minnesota, USA; 2.2 g weight, 1.4 cc and 5 cm pressure catheter length) was used. With mice positioned in dorsal recumbency, a 1-cm incision was made through the skin along the ventral neck midline. The pressure catheter was introduced through the carotid artery to the aortic arch. The transmitter body was then placed subcutaneously inside a pocket created on the dorsal aspect of the animal, allowing for comfortable and unobtrusive motion range. After verification of systemic BP signals, the incision was closed using 4-0 non-absorbable suture with a simple interrupted pattern.

Acclimatization, Blood Pressure Recordings, and Sleep Fragmentation

After recovery from surgery for ≥ 10 days, mice were transferred to the sleep fragmenter device for habituation to the cage and the sweeper bar. The recording cages were mounted on a DSI telemetry receiver (RPC-1), which was in turn connected to an acquisition computer through a data exchange matrix. After at least an additional week of acclimatization, the magnetic switch of the transmitter was activated, and BP recordings were begun at 07:00 (shown as time 0 in Figure 1). Systolic and diastolic data were continuously acquired for 24 h using Dataquest ART acquisition software (DSI, St Paul, Minnesota, USA; version 3.1) at multiple intervals until 20 weeks SF exposures were completed.

Food Consumption

Food consumption per cage was registered daily, always at the same time of the day (middle of the light period). Animal food consumption was then calculated by dividing the daily cage chow utilization by the number of mice in the cage

Elastic Fiber Disruption and Disorganization in Aorta Wall

Cross-sections of aortas were performed (n = 10 for the aortic arch and n = 10 for the thoracic aorta) and embedded in paraffin. Sections were stained with hematoxylin and eosin (H&E) for morphology overview, and with Elastica Van Gieson (EVG) for elastic fiber analysis. All sections were captured with a digital color camera mounted on a microscope (Nikon E300, Nikon USA, Melville, NY). The grade of elastic lamina disruption and disorganization of the aorta was evaluated using the following criteria: disruption referred to the complete fragmentation of one elastic fiber area; disorganization referred to the inability to count the amount of organized elastic fibers. These patterns were quantified by an investigator who was blinded to the identity of the sections.

Aortic Lumen Area and Aortic Wall Thickness Quantification

ImageJ software was used to analyze the relative lumen area and the relative wall thickness in both arch and thoracic aorta sections. Similarly, these analyses were performed by a blinded investigator.

Quantitative Analysis of Aortic Atherosclerotic Lesions

Aorta dissection and preservation was carried out as previously described by Subbarao and colleagues.[19] Briefly, the

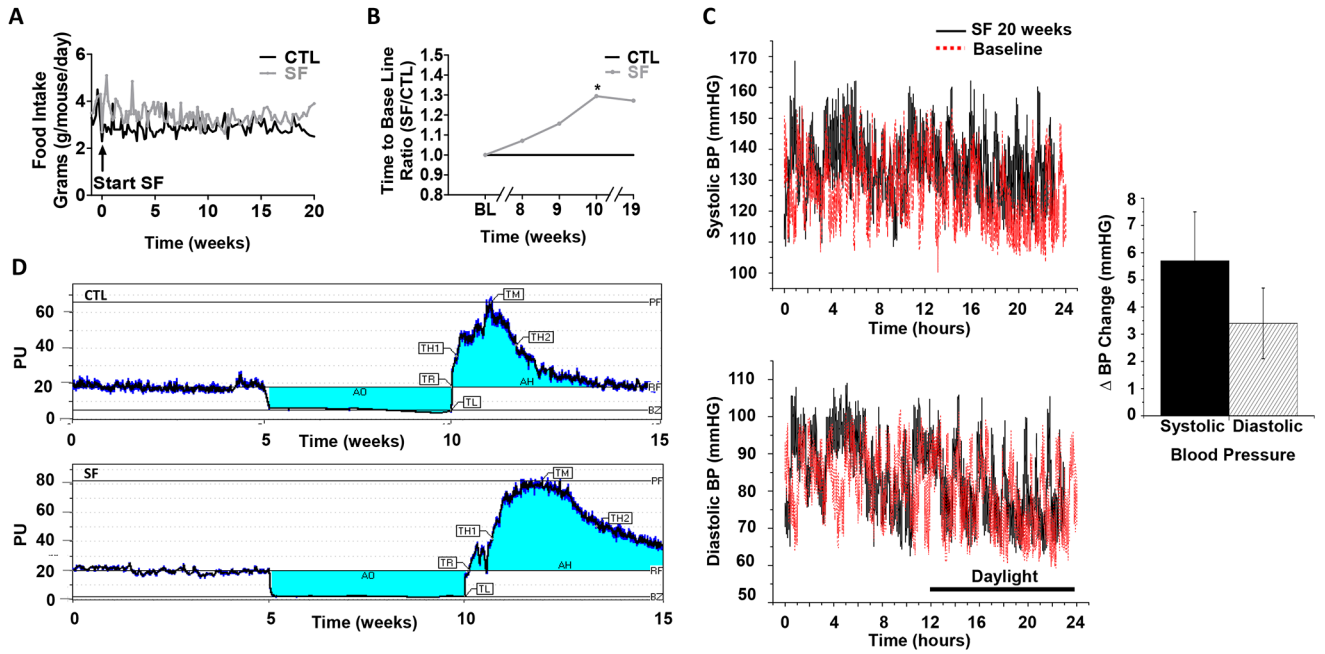

Figure 1—Food intake, endothelial function and blood pressure. **(A)** SF-induced hyperphagic behavior. C57BL/6J mice exposed to SF consumed more food on a daily basis over the 20-week period in comparison with CTL (n = 15/group). Data are expressed in grams of chow consumed per mouse per day. **(B)** Post-occlusive hyperemic response. Time to reach baseline perfusion levels during the post-occlusive period at time points 8, 9, 10, and 19 weeks of SF exposure (ratio between SF and CTL groups at each time point; SF vs. CTL – $P < 0.03$) (n = 15/group). **(C)** Representative 24-h blood pressure recordings in mmHg (upper tracing – systolic BP and lower tracings – diastolic BP at baseline (red lines) and following 20-week SF-exposures (black lines). Time 12-24 indicates daylight period. Bar graph indicates mean increases in systolic and diastolic BP in 3 mice following SF ($P < 0.05$ SF vs. baseline or CTL). **(D)** Post-occlusive hyperemic response. Representative example for the 3 phases of a laser Doppler post-occlusive hyperemic response test in mice exposed to SF and CTL conditions. AO, occlusion area; AH, hyperemia area; TL, time to latency; TR, time to recovery; TH1, time to half before hyperemia; TH2, time to half after hyperemia; TM, time to max; PF, peak flow; RF, rest flow; BZ, biological zero; PU, perfusion units.

aortas of 5 mice in each experimental group were en face pinned-out and stained with Sudan IV for evaluation of gross atherosclerotic lesions.

Immune Cells and Senescence Markers Detection in Aortic Tissue

Senescent cells differ from other non-dividing (quiescent, terminally differentiated) cells in several ways, although no single feature of the senescent phenotype is exclusively specific. Hallmarks of senescent cells include among others, irreversible growth arrest, reduced expression of telomerase reverse transcriptase (TERT) and increased expression of cyclin-dependent kinase inhibitor 2A (p16INK4a), as well as robust secretion of numerous growth factors and cytokines, such as keratinocyte chemoattractant/chemokine (C-X-C motif) ligand 1 (KC/CXCL1) and interleukin 6 (IL-6), proteases, and other proteins, such as cyclin D1, cyclin A, or insulin-like growth factor-binding protein 3 (IGFBP3), the latter also designated as senescence-associated secretory phenotypes (SASPs). To assess for the presence of SASPs, aortic roots were embedded in OCT, snap-frozen in liquid nitrogen and serial 5-µm thick cryosections were performed before immunostaining. Histological localization of immune cells and senescence markers was performed under bright field microscope. Ascending aorta cryosections were stained with Oil Red O and counterstained with hematoxylin for foam cell detection. Sections used for macrophage and senescence markers detection were fixed in acetone for 6 min at room temperature, air dried for 30 sec, rinsed with distilled water, and boiled for 30 min in 0.01M citrate buffer (pH 6.0). Adjacent sections were incubated for 1 h at room temperature with rat anti-F4/80 (Biolegend, San Diego, CA, USA; 1:500) for macrophage detection; rabbit anti-P16-INK4A, rabbit anti-cyclin D1, rabbit anti-TERT (Bioss Inc, Woburn, MA, USA; 1:500), or rabbit anti-cyclin A (Abcam, Cambridge, MA, USA; 1:500) antibody for senescence cell phenotype detection in PBS containing 1% BSA and 0.2% Triton X-100. Antibodies were detected with a peroxidase-chromogen system (Vector Laboratories, Burlingame, CA, USA), and finally sections were counterstained with hematoxylin and eosin. All aorta images were captured with a digital color camera mounted on a microscope (Nikon E300, Nikon USA, Melville, NY).

KC/CXCL1, IL-6, and IGFBP3 Plasma Levels

After 20 weeks of SF exposure or CTL conditions, plasma samples were analyzed for senescence markers using enzyme-linked immunosorbent assay (ELISA) kits according to the manufacturer's protocol. The appropriate range of the KC/CXCL1 assay (RayBiotech, Inc. Norcross, GA, USA) was 1 pg/mL to 150 pg/mL, with detection limit at 1 pg/mL, and intra- and inter-individual coefficients of variation up to < 10% and < 12%, respectively. Similarly, the minimum detectable concentration of IL-6 (Biolegend, San Diego, CA, USA) was 2 pg/mL, with an intra-assay precision up to 5.7% and an inter-assay precision up to 10.7%. Finally, IGFBP3 mouse ELISA kit (Abcam, Cambridge, MA, USA) presented a minimum

detectable concentration < 45 pg/mL with an appropriate detection range of 55 pg/mL to 40,000 pg/mL. The intra-assay variation coefficient (CV) was up to 10% and < 12% of inter-assay CV. All ELISA kits used showed no cross-reactivity with wide range of cytokines, as tested by the manufacturer.

Statistical Analysis

All values are expressed as mean ± standard error (SEM). Analyses of variance procedures followed by post hoc tests and Student *t*-tests were used to compare the results between SF and CTL groups. In all cases, two-tailed P value of < 0.05 was considered to achieve statistical significance.

RESULTS

Food Intake

As previously reported,[20] mice exposed to SF exhibited increased food intake that began within a few days after the initiation of SF and was sustained throughout the duration of the 20 weeks SF exposure (Figure 1A). At the end of SF exposures, the overall incremental weight changes associated with SF were 3.2 ± 1.2 g when compared to CTL (P < 0.05).

Endothelial Function Testing

Laser-Doppler analysis of dorsal tail vein blood flow did not reveal significant differences in resting blood flow between SF and SC groups at any of the weekly time points. The time latency between occlusion release and peak reperfusion flow (Tmax) did not change over time. However, both peak flow (as % of baseline) and time to return to baseline perfusion values were altered in SF-exposed mice. Indeed, SF mice showed increased duration of post-occlusive hyperemic responses, starting at week 8 of exposure and thereafter (Figure 1B and 1C; n = 10/group; P < 0.03).

Systemic Blood Pressure and Heart Rate Measurements

Systolic and diastolic BP were measured for 24 h period at baseline (before starting SF) and after 2, 6, 8, 12, 16, 18, and 20 weeks of SF exposures in an separate group of animals (n = 6). As shown in Figure 1C, starting at week 8 and concluding at week 12, all mice exposed to SF exhibited higher systolic and diastolic BP values throughout the day, particularly during the daylight hours (shown as time 0-12 hours) when compared to pre-SF conditions or to CTL mice (data not shown). The mean increment in systolic BP associated with SF was 5.7 ± 1.8 mm Hg and 3.4 ± 1.3 mm Hg for diastolic BP (P < 0.05). Of note, increases in heart rate (HR) were apparent after induced arousals during the initial phases of SF (mean HR increases of 32 ± 12 bpm during the first week of SF) but were usually void of concomitant increases in BP. Furthermore, progressive disappearance of the chronotropic effect of arousals was noted over time, such that no significant changes in HR were noticeable following 4 weeks of SF and thereafter.

Atherosclerotic Lesion Formation

En face analysis of SF-exposed and CTL aortas showed no evidence of macroscopically recognizable lesion formation (either atherosclerotic plaques or lipid accumulation) (Figure 2A; n = 5/group). However, significant elastic fiber disruption (arch aorta: 2.75 ± 0.25 in CTL vs. 16.38 ± 1.89 in SF, P < 0.01; thoracic aorta: 4.67 ± 1.67 in CTL vs. 13.75 ± 1.20 in SF, n = 10/group; P < 0.01) and fiber disorganization were apparent in SF-exposed mice (Figure 2B and 2E; P < 0.01). Despite the elastic fiber alterations, no significant differences emerged in either aortic wall thickness (aortic arch: 39.66% ± 1.63% in CTL vs. 36.49% ± 1.42% in SF; thoracic aorta: 36.80% ± 0.25% in CTL vs. 38.33% ± 1.70% in SF) or in aortic lumen (aortic arch: 60.35% ± 1.63% in CTL vs. 63.51% ± 1.42% in SF; thoracic aorta: 63.20% ± 0.25% in CTL vs. 61.67% ± 1.70% in SF; Figure 2C and 2D).

Immune Cells Recruitment into the Aorta Wall

Mice exposed to SF showed increased infiltration of foam cells and macrophages in the aortic wall compared to CTL mice, particularly in the aortic root sections (Figure 3A). Unbiased counts over 3 sections/animal revealed a 3.7 fold increase in F4/80 cells (n = 7 mice/group; P < 0.01) and a 4.3 fold increase in foam cell counts (n = 7 mice/group; P < 0.01).

Senescence Markers

In SF-exposed mice, increases in p16INK4a expression (Figure 3A) in aortic root sections, as well as significantly increased plasma IL-6 levels (Figure 3C) emerged in 20 weeks SF-exposed mice compared to CTL animals. Compatible with increased senescence, SF-exposed mice also showed decreased expression in TERT and cyclin A (Figure 3A), whereas no differences in cyclin D1 (Figure 3A) expression or in KC/CXCL1 (Figure 3B) and IGFBP3 (Figure 3D) plasma levels occurred.

DISCUSSION

This study shows that long-term SF exposures imposed during the circadian time window associated with the preferential sleep period in mice lead to the emergence of endothelial dysfunction emerging around week 8-9 of SF exposures, and manifesting as delayed post-occlusive reperfusion kinetics. Furthermore, minor, albeit significant, increases in systemic BP emerge around the same timeframe. Analysis of aortas after 20 weeks of SF revealed that no increases in fat deposition were apparent in the macroscopic assessments of *en face* aorta using Sudan IV staining and increased in the number of foam cells were located in the vessel walls. Furthermore, increased numbers of activated macrophages along with elevated IL-6 levels, and altered expression of SASPs were present in SF-exposed mice, and are suggestive of an increased propensity for an accelerated atherosclerosis phenotype. Strikingly, the overall collagen fiber structural arrangement of the vascular wall was markedly disrupted with both increased disorganization and frequency of disrupted continuity of the fibrillar structures, compatible not only with potential alterations in collagen subtypes, but also with the increased senescence of the cellular substrate in the vessel wall, as evidenced by increased expression of p16INK4a and reduced expression of TERT and cyclin A.[21-25]

Before we discuss the potential implications of our findings, some methodological considerations merit particular mention. First, the sleep fragmentation procedures used herein afford several advantages, namely reproducibility, lack of measurable increases in stress hormones, absence of human contact, and preserved social setting and food and water access,[16] all of

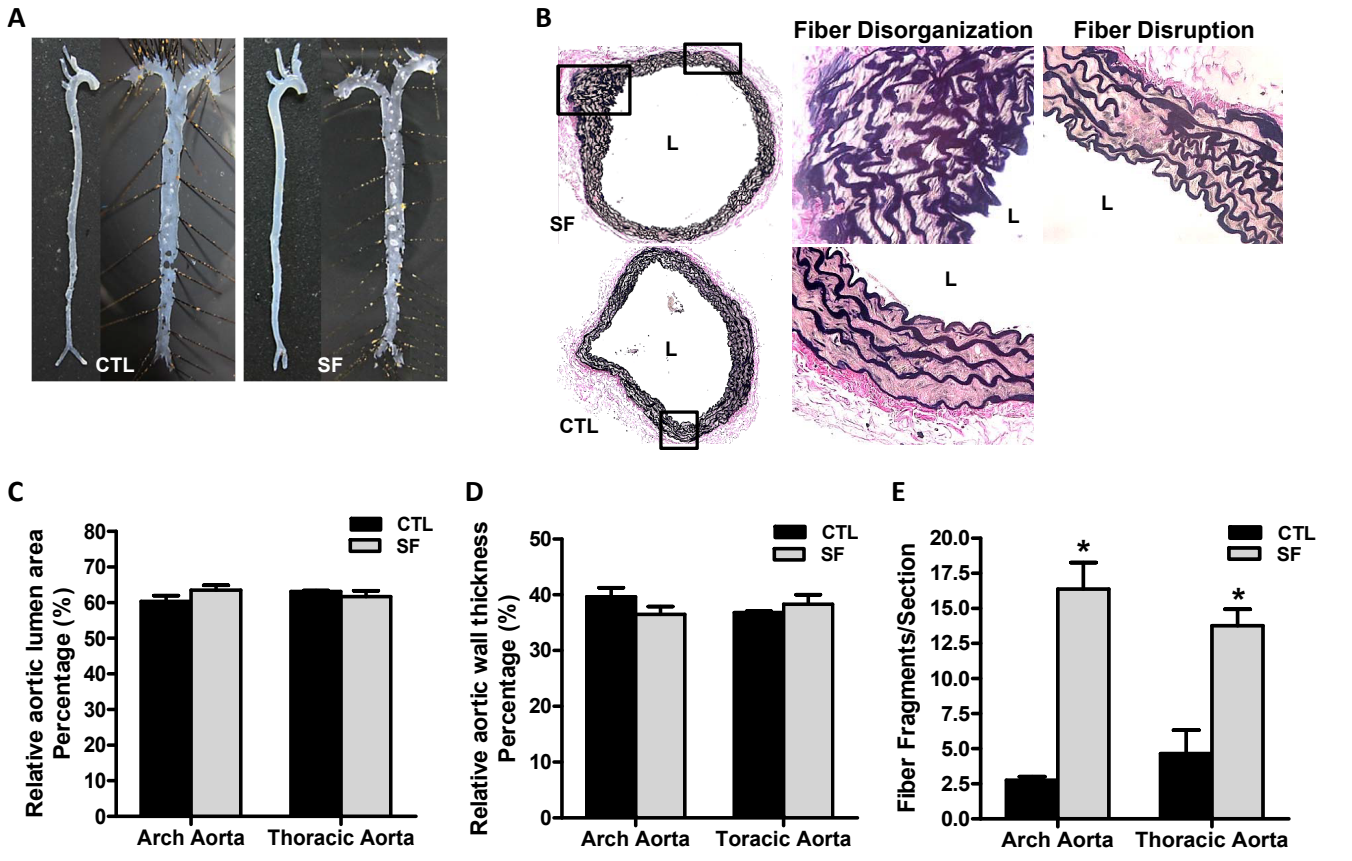

Figure 2—Aortic structural changes associated with long-term SF. **(A)** Representative e*n face* analysis of aortas from mice after 20-weeks SF exposures and CTL conditions (n = 5/group) using Sudan IV staining. **(B)** EVG staining for detection of elastic fiber disorganization and elastic fiber disruption on aorta arch from SF and CTL exposed mice. **(C)** Relative vessel luminal area in aortic arch and thoracic aorta after 20 weeks of SF exposures or CTL conditions (%). **(D)** Relative aortic wall thickness in aortic arch and thoracic aorta after 20 weeks SF exposures vs. CTL mice (%). **(E)** Number of fragmented elastic fibers per section after 20 weeks of SF and CTL exposures. * P < 0.01, SF vs. CTL.

which could independently contribute to vascular dysfunction. Furthermore, we have also shown that the current model of SF does not curtail sleep duration, and that the episodic arousals in the context of preserved sleep duration primarily manifest as increased sleep propensity, a major clinical symptom in OSA patients.[11] However, neither the current SF paradigm, nor other existing SF-inducing methodologies exactly mimic the arousal processes operative during apneic episodes. Furthermore, we are unaware of any other studies in which the duration of SF exceeded 2 weeks. This is an important issue since even though altered glucose homeostasis is present after 2 weeks of SF, no changes in body weight are apparent.[20,26] We should also point out that chronic SF induces increases in central nervous system levels of tumor necrosis factor-α (TNF-α),[11,27] and it is possible that increased systemic levels of this cytokine may operate also as a potent atherogenic pro-inflammatory agent, most likely via its TNF p75 receptor.[28,29] Similarly, we have previously shown that long-term SF induces activation of NADPH oxidase and increased oxidative stress,[10,30] both of which are major pathophysiological mechanisms underlying vascular dysfunction and atherosclerosis.[31-33] Therefore, it is possible that upstream processes such as inflammation and oxidative stress may initiate endothelial dysfunction through activation of monocyte-endothelial interactions, leading to the increased formation of foam cells observed here.[34] Additionally, the intra- and inter-individual reproducibility of the post-occlusive hyperemic responses was assessed in preliminary experiments, and exhibited highly satisfactory consistency with high intra-class correlation coefficients (data not shown). Thirdly, we should stress that we opted not to implement administration of an atherogenic diet or to employ transgenic mice with heightened susceptibility to atherogenesis, since we wished to examine the isolated contribution of SF on the vasculature. In this context, Savransky and colleagues adopted a similar approach when they examined the role of chronic intermittent hypoxia, another key feature of sleep apnea, on the generation and propagation of atherosclerosis in mice.[35] Furthermore, exposures to high cholesterol diet in the absence of other perturbations were not associated with increased atherogenesis in mice. We are also unaware of any studies in which the incremental weight gain that occurred in current SF-exposed mice can be accomplished using normal chow diet, such that the relative absence of extensive atheromatous lesions in the aortic wall was overall anticipated. Fourthly, the increased orexigenic behaviors during SF were sustained throughout the exposures and accompanied by modest, albeit significant weight gain. Although we cannot determine with certainty whether the changes in body weight underlie the vascular changes reported herein, we are unable

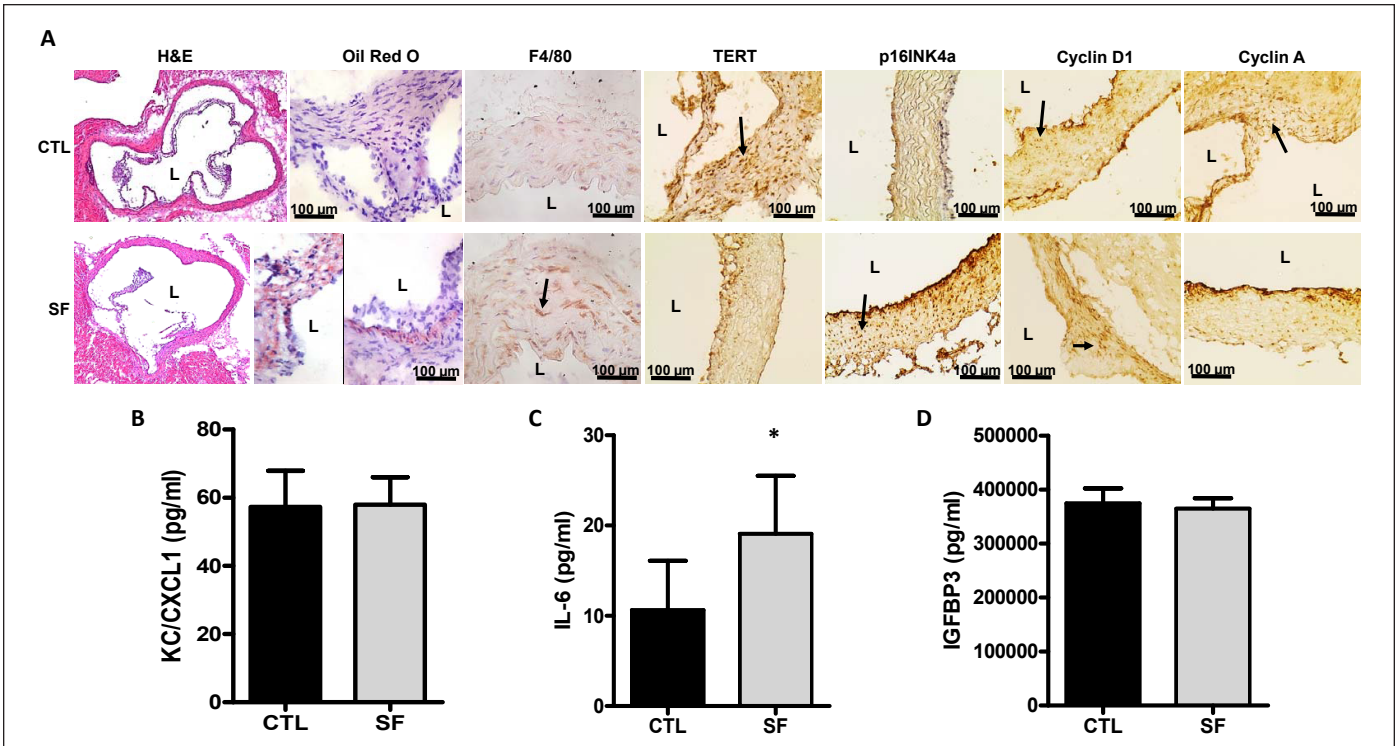

Figure 3—Inflammatory cell recruitment and cell senescence markers in aorta following long-term SF. **(A)** SF and CTL root aortas were cryosectioned and stained with H&E for morphology and Oil Red O for foam cell detection. Consecutive cryosections were immunostained with monoclonal antibodies for detection of macrophages (F4/80) and senescence markers (TERT, p16INK4a, cyclin D1, cyclin A). Arrows indicate examples of labeled cells for each of the selected markers. **(B)** Plasma levels of SASPs KC/CXCL1 (pg/mL), **(C)** IL-6 (pg/mL) and **(D)** IGFBP3 (pg/mL) after 20 weeks of SF. * $P < 0.01$, SF vs. CTL.

to either confirm or dispel such possibility under the current study design. However, we should remark that no evidence of atherosclerotic lesions emerged after 20 weeks of feeding with high cholesterol diet in mice,[36] leading us to postulate that the changes in vascular functions are most likely ascribable to SF, rather than to the increased weight induced by SF while feeding the mice with regular chow. Finally, the observational nature of the present study is acknowledged, even though efforts were made to identify potential leads on mechanisms that will have to be explored in the future.

Our experiments conclusively show that long-term sleep fragmentation, as might occur in multiple sleep disorders, particularly in sleep disordered breathing, is potentially an important contributor to the cardiovascular morbidity of these conditions.[37,38] Indeed, we found the presence of altered endothelial function as represented by delayed post-occlusive hyperemia, and such findings are remarkably analogous to those reported by our group and by others in both children and adults with sleep apnea.[39-43] It is possible that the recurrent arousals may promote enhanced sympathetic activation that will in turn lead to elevations in systemic BP along with disruption of endothelial integrity.[44-48] Future exploration on the roles of disrupted central and peripheral autonomic nervous system function and their potential pathways to deregulate BP control and vascular integrity in the context of fragmented sleep are clearly justified based on current results.

The integrity of the elastic properties and structural arrangements in the vessel wall is an integral component to the preservation of vascular health. Perturbations in the continuity of the internal elastic lamina with disruption of the elastic fiber arrangements have been previously implicated in the early phases of atherosclerosis in apolipoprotein E null mice.[49] Potential imbalances in the extracellular matrix elements of the vessel, and of elastic fibers in particular, are apparent even during early atherogenesis, with elastin emerging as a critical regulatory molecule that regulates the phenotypic modulation, proliferation, and migration of smooth muscle cells in the vessel wall.[49] Furthermore, denatured arterial elastin by cholesterol accumulation becomes susceptible to proteolytic enzymes such as elastase and matrix metalloproteinases, thereby reducing vessel wall elasticity and potentially promoting hypertension.[22] Here we show that in the absence of alterations in aortic wall thickness or luminal patency, long-term SF induced major disruption of elastic fiber architecture, highly suggestive of early features of atherosclerosis, despite preservation of normal chow diet in *a priori* a relatively susceptible wild-type mouse strain (i.e., C57/Bl6).[50-54]

Cellular senescence, the irreversible growth arrest of mitotic cells has been proposed as a common mechanism underlying vascular dysfunction associated with aging processes.[55,56] Improved understanding of the molecular changes associated with cellular senescence has yielded panels of robust biomarkers for detecting senescence in cells, such as changes in the expression of telomere-dependent (e.g., TERT) and telomere-independent markers (e.g., p16INK4a and cyclin A).[6] The degree of global transcriptional alteration during senescence leads to altered secretomes, termed the SASPs as evidenced by increases in the secretion of pro-inflammatory cytokines, proteases, and growth factors, all of which coordinate a sustained low-grade inflammatory state that further accelerates vascular

dysfunction.[21-25,57,58] In our studies, long-term SF was associated with not only increased plasma levels of IL-6, a frequent occurrence in both adult and pediatric patients with OSA,[59,60] but also with increased evidence for SASPs, suggesting that chronic sleep perturbations induced increased senescence of cells within the vessel wall that may further contribute to vascular dysfunction. Taken together, current findings support the notion that diseases associated with substantial and prolonged SF, such as OSA, induce and accelerate atherogenesis via multiple pathways that involve recruitment of inflammatory processes, disruption of structural vessel wall integrity, and activation of senescence secretomes, all of which may coordinate vascular aging and dysfunction.

Significance

The results of the present study demonstrate that long-term sleep fragmentation induces vascular endothelial dysfunction and it is also associated with morphologic vessel changes characterized by elastic fiber disruption and disorganization. Furthermore, the increased recruitment of inflammatory cells to the wall and altered expression of senescence markers are further supportive of a putative mechanism for the effects of sleep fragmentation on endothelial dysfunction and structural vascular changes. These findings may have substantial implications for the understanding of vascular regulation and deregulation in diseases associated with sleep fragmentation, such as in sleep apnea.

ACKNOWLEDGMENTS

Authors' contributions: Dr. Carreras participated in the conceptual framework of the project, performed experiments, analyzed data, and drafted components of the manuscript. Dr. Zhang, Mr. Peris, Dr. Qiao, Dr. Gileles-Hillel, and Dr. Li performed experiments. Dr. Wang drafted portions of the manuscript and served as blinded observer. Dr. Gozal conceptualized the project, provided critical input in all phases of the experiments, analyzed data, drafted the ulterior versions of the manuscript, and is responsible for the financial support of the project and the manuscript content. All authors have reviewed and approved the final version of the manuscript.

DISCLOSURE STATEMENT

This was not an industry supported study. This work was supported by the National Institutes of Health (HL-65270, HL-086662, HL-107160 to Dr. Gozal) and the Comer Kids Classic grant (to Dr. Zhang). The other authors have indicated no financial conflicts of interest.

REFERENCES

1. Gozal D, Capdevila OS, Kheirandish-Gozal L. Metabolic alterations and systemic inflammation in obstructive sleep apnea among nonobese and obese prepubertal children. Am J Respir Crit Care Med 2008;177:1142-9.
2. O'Brien LM, Holbrook CR, Mervis CB, et al. Sleep and neurobehavioral characteristics of 5- to 7-year-old children with parentally reported symptoms of attention-deficit/hyperactivity disorder. Pediatrics 2003;111:554-63.
3. Patil SP, Schneider H, Schwartz AR, Smith PL. Adult obstructive sleep apnea: pathophysiology and diagnosis. Chest 2007;132:325-37.
4. Young T, Palta M, Dempsey J, Skatrud J, Weber S, Badr S. The occurrence of sleep-disordered breathing among middle-aged adults. N Engl J Med 1993;328:1230-5.
5. Farre R, Montserrat JM, Navajas D. Morbidity due to obstructive sleep apnea: insights from animal models. Curr Opin Pulm Med 2008;14:530-6.
6. Atkeson A, Jelic S. Mechanisms of endothelial dysfunction in obstructive sleep apnea. Vasc Health Risk Manag 2008;4:1327-35.
7. Kohler M, Stradling JR. Mechanisms of vascular damage in obstructive sleep apnea. Nat Rev Cardiol 2010;7:677-85.
8. Mullington JM, Haack M, Toth M, Serrador JM, Meier-Ewert HK. Cardiovascular, inflammatory, and metabolic consequences of sleep deprivation. Progr Cardiovasc Dis 2009;51:294-302.
9. Kim J, Hakim F, Kheirandish-Gozal L, Gozal D. Inflammatory pathways in children with insufficient or disordered sleep. Respir Physiol Neurobiol 2011;178:465-74.
10. Nair D, Zhang SX, Ramesh V, et al. Sleep fragmentation induces cognitive deficits via nicotinamide adenine dinucleotide phosphate oxidase-dependent pathways in mouse. Am J Respir Crit Care Med 2011;184:1305-12.
11. Ramesh V, Nair D, Zhang SX, et al. Disrupted sleep without sleep curtailment induces sleepiness and cognitive dysfunction via the tumor necrosis factor-alpha pathway. J Neuroinflammation 2012;9:91.
12. Kaushal N, Ramesh V, Gozal D. Human apolipoprotein E4 targeted replacement in mice reveals increased susceptibility to sleep disruption and intermittent hypoxia. Am J Physiol Regul Integr Comp Physiol 2012;303:R19-29.
13. Huber R, Deboer T, Tobler I. Effects of sleep deprivation on sleep and sleep EEG in three mouse strains: empirical data and simulations. Brain Res 2000;857:8-19.
14. Ramesh V, Thatte HS, McCarley RW, Basheer R. Adenosine and sleep deprivation promote NF-kappaB nuclear translocation in cholinergic basal forebrain. J Neurochem 2007;100:1351-63.
15. McKenna JT, Tartar JL, Ward CP, et al. Sleep fragmentation elevates behavioral, electrographic and neurochemical measures of sleepiness. Neuroscience 2007;146:1462-73.
16. Ramesh V, Kaushal N, Gozal D. Sleep fragmentation differentially modifies EEG delta power during slow wave sleep in socially isolated and paired mice. Sleep Sci 2009;2:64-75.
17. Wahlberg E, Olofsson P, Swendenborg J, Fagrell B. Changes in postocclusive reactive hyperaemic values as measured with laser Doppler fluxmetry after infrainguinal arterial reconstructions. Eur J Vasc Endovasc Surg 1995;9:197-203.
18. Kheirandish-Gozal L, Bhattacharjee R, Kim J, Clair HB, Gozal D. Endothelial progenitor cells and vascular dysfunction in children with obstructive sleep apnea. Am J Respir Crit Care Med 2010;182:92-7.
19. Subbarao K, Jala VR, Mathis S, et al. Role of leukotriene B4 receptors in the development of atherosclerosis: potential mechanisms. Arterioscler Thromb Vasc Biol 2004;24:369-75.
20. Wang Y, Carreras A, Lee S, et al. Chronic sleep fragmentation promotes obesity in young adult mice. Obesity 2014;22:758-62.
21. Cardenas JC, Owens AP 3rd, Krishnamurthy J, Sharpless NE, Whinna HC, Church FC. Overexpression of the cell cycle inhibitor p16INK4a promotes a prothrombotic phenotype following vascular injury in mice. Arterioscler Thromb Vasc Biol 2011;31:827-33.
22. Vafaie F, Yin H, O'Neil C, et al. Collagenase-resistant collagen promotes mouse aging and vascular cell senescence. Aging Cell 2014;13:121-30.
23. Gizard F, Heywood EB, Findeisen HM, et al. Telomerase activation in atherosclerosis and induction of telomerase reverse transcriptase expression by inflammatory stimuli in macrophages. Arterioscler Thromb Vasc Biol 2011;31:245-52.
24. Gizard F, Nomiyama T, Zhao Y, et al. The PPARalpha/p16INK4a pathway inhibits vascular smooth muscle cell proliferation by repressing cell cycle-dependent telomerase activation. Circ Res 2008;103:1155-63.
25. Maziere C, Trecherel E, Ausseil J, Louandre C, Maziere JC. Oxidized low density lipoprotein induces cyclin A synthesis. Involvement of ERK, JNK and NFkappaB. Atherosclerosis 2011;218:308-13.
26. Baud MO, Magistretti PJ, Petit JM. Sustained sleep fragmentation affects brain temperature, food intake and glucose tolerance in mice. J Sleep Res 2013;22:3-12.
27. Kaushal N, Ramesh V, Gozal D. TNF-alpha and temporal changes in sleep architecture in mice exposed to sleep fragmentation. PloS One 2012;7:e45610.
28. Gao X, Belmadani S, Picchi A, et al. Tumor necrosis factor-alpha induces endothelial dysfunction in Lepr(db) mice. Circulation 2007;115:245-54.

29. Schreyer SA, Peschon JJ, LeBoeuf RC. Accelerated atherosclerosis in mice lacking tumor necrosis factor receptor p55. J Biol Chem 1996;271:26174-8.
30. Zhang SX, Khalyfa A, Wang Y, et al. Sleep fragmentation promotes NADPH oxidase 2-mediated adipose tissue inflammation leading to insulin resistance in mice. Int J Obes (Lond) 2014;38:619-24.
31. Gage MC, Yuldasheva NY, Viswambharan H, et al. Endothelium-specific insulin resistance leads to accelerated atherosclerosis in areas with disturbed flow patterns: a role for reactive oxygen species. Atherosclerosis 2013;230:131-9.
32. Kinoshita H, Matsumura T, Ishii N, et al. Apocynin suppresses the progression of atherosclerosis in apoE-deficient mice by inactivation of macrophages. Biochem Biophys Res Commun 2013;431:124-30.
33. Violi F, Pignatelli P, Pignata C, et al. Reduced atherosclerotic burden in subjects with genetically determined low oxidative stress. Arterioscler Thromb Vasc Biol 2013;33:406-12.
34. Jia Z, Babu PV, Si H, et al. Genistein inhibits TNF-alpha-induced endothelial inflammation through the protein kinase pathway A and improves vascular inflammation in C57BL/6 mice. Int J Cardiol 2013;168:2637-45.
35. Savransky V, Nanayakkara A, Li J, et al. Chronic intermittent hypoxia induces atherosclerosis. Am J Respir Crit Care Med 2007;175:1290-7.
36. Song D, Fang G, Mao SZ, Ye X, Liu G, Gong Y, Liu SF. Chronic intermittent hypoxia induces atherosclerosis by NF-κB-dependent mechanisms. Biochim Biophys Acta 2012;1822:1650-9.
37. Cuellar NG. The effects of periodic limb movements in sleep (PLMS) on cardiovascular disease. Heart Lung 2013;42:353-60.
38. Sanchez-de-la-Torre M, Campos-Rodriguez F, Barbe F. Obstructive sleep apnoea and cardiovascular disease. Lancet Respir Med 2013;1:61-72.
39. Gozal D, Kheirandish-Gozal L, Serpero LD, Sans Capdevila O, Dayyat E. Obstructive sleep apnea and endothelial function in school-aged nonobese children: effect of adenotonsillectomy. Circulation 2007;116:2307-14.
40. Lurie A. Endothelial dysfunction in adults with obstructive sleep apnea. Adv Cardiol 2011;46:139-70.
41. Kheirandish-Gozal L. The endothelium as a target in pediatric OSA. Front Neurol 2012;3:92.
42. Lavie L. Oxidative stress inflammation and endothelial dysfunction in obstructive sleep apnea. Front Biosci 2012;4:1391-403.
43. Kaczmarek E, Bakker JP, Clarke DN, et al. Molecular biomarkers of vascular dysfunction in obstructive sleep apnea. PloS One 2013;8:e70559.
44. Meerlo P, Sgoifo A, Suchecki D. Restricted and disrupted sleep: effects on autonomic function, neuroendocrine stress systems and stress responsivity. Sleep Med Rev 2008;12:197-210.
45. Chouchou F, Pichot V, Pepin JL, et al. Sympathetic overactivity due to sleep fragmentation is associated with elevated diurnal systolic blood pressure in healthy elderly subjects: the PROOF-SYNAPSE study. Eur Heart J 2013;34:2122-31, 31a.
46. Kuo TB, Lai CT, Chen CY, Lee GS, Yang CC. Unstable sleep and higher sympathetic activity during late-sleep periods of rats: implication for late-sleep-related higher cardiovascular events. J Sleep Res 2013;22:108-18.
47. Hakim F, Gozal D, Kheirandish-Gozal L. Sympathetic and catecholaminergic alterations in sleep apnea with particular emphasis on children. Front Neurol 2012;3:7.
48. Perry JC, Bergamaschi CT, Campos RR, Andersen ML, Casarini DE, Tufik S. Differential sympathetic activation induced by intermittent hypoxia and sleep loss in rats: Action of angiotensin (1-7). Auton Neurosci 2011;160:32-6.
49. Jones GT, Jiang F, McCormick SP, Dusting GJ. Elastic lamina defects are an early feature of aortic lesions in the apolipoprotein E knockout mouse. J Vasc Res 2005;42:237-46.
50. Ooyama T, Sakamato H. Elastase in the prevention of arterial aging and the treatment of atherosclerosis. Ciba Found Symp 1995;192:307-17; discussion 18-20.
51. Seyama Y, Wachi H. Atherosclerosis and matrix dystrophy. J Atheroscler Thromb 2004;11:236-45.
52. Maeda I, Kishita S, Yamamoto Y, et al. Immunochemical and immunohistochemical studies on distribution of elastin fibres in human atherosclerotic lesions using a polyclonal antibody to elastin-derived hexapeptide repeat. J Biochem 2007;142:627-31.
53. Chan EC, Jones GT, Dusting GJ, Datla SR, Jiang F. Prevention of aortic elastic lamina defects by losartan in apolipoprotein(E)-deficient mouse. Clin Exp Pharmacol Physiol 2009;36:919-24.
54. Paigen B, Ishida BY, Verstuyft J, Winters RB, Albee D. Atherosclerosis susceptibility differences among progenitors of recombinant inbred strains of mice. Arteriosclerosis 1990;10:316-23.
55. Burton DG, Matsubara H, Ikeda K. Pathophysiology of vascular calcification: Pivotal role of cellular senescence in vascular smooth muscle cells. Exp Gerontol 2010;45:819-24.
56. Bailey-Downs LC, Tucsek Z, Toth P, et al. Aging exacerbates obesity-induced oxidative stress and inflammation in perivascular adipose tissue in mice: a paracrine mechanism contributing to vascular redox dysregulation and inflammation. J Gerontol A Biol Sci Med Sci 2013;68:780-92.
57. Kuilman T, Peeper DS. Senescence-messaging secretome: SMS-ing cellular stress. Nat Rev Cancer 2009;9:81-94.
58. Franceschi C, Bonafe M, Valensin S, et al. Inflamm-aging. An evolutionary perspective on immunosenescence. Ann N Y Acad Sci 2000;908:244-54.
59. Gozal D, Serpero LD, Sans Capdevila O, Kheirandish-Gozal L. Systemic inflammation in non-obese children with obstructive sleep apnea. Sleep Med 2008;9:254-9.
60. Nadeem R, Molnar J, Madbouly EM, et al. Serum inflammatory markers in obstructive sleep apnea: a meta-analysis. J Clin Sleep Med 2013;9:1003-12.